Multi response Particle Swarm Optimization of Wire Electro Discharge Machining parameters of Nitinol alloys

Mohammed Yunus (yunus.mohammed@rediffmail.com)
Umm Al-Qura University https://orcid.org/0000-0003-1116-4978
Mohammad S. Alsoufi
Umm Al-Qura University College of Engineering and Islamic Architecture

Research

Keywords: WEDM, Material removal rate, Surface finish, Particle swarm optimization, Nitinol alloy

Posted Date: July 2nd, 2020

DOI: https://doi.org/10.21203/rs.3.rs-38245/v1

Abstract

The conventional process of Machining of Nitinol alloy leads to extensive wear on the tool and deprived surface quality. Wire electro discharge machining (WEDM) is widely accepted for machining this alloy involving various input factors, namely, P, (pulse-on-duration), Q, (pulse-off-duration), C, (maximum-current), and V, (voltage). The factor's effect on MRR (metal removal rate) and SR (surface roughness) responses and multi-response optimization of the WEDM process by employing PSO (particle swarm optimization) method are studied. The relationship model between factors and response characteristics were generated by ANOVA and optimized by response surface methodology has shown more significant factors (A and C). Though the effect of WEDM process factors on SR and MRR are contradictory when studied individually. MRPSO method was employed to get the best optimum condition for minimizing SR and maximizing MRR. MRPSO results improved the responses for vast combination of optimal setting of factors to meet the product requirements.

Introduction

The present development of science and technology demands the parts made of materials having strong (higher strength) and lightweight (low density) in the form of newer materials. Various alloys are available, especially the combination of Nickel and Titanium forms Nitinol alloy has been widely used as one of such favorable metal possessing the desired properties. These properties shape remembering effect, pseudo adaptability, creep, and corrosion resistance, etc. along with them adding other blending material such as Cu enhances phase changing temperature levels, immediate response to stimulation, cyclic, and vibration damping characteristics. These alloys are innovative metallic alloys find their applications mostly in aerospace and automobile fields, medicinal as well as dental fields [1]. Apart from the above said major fields. Their direct application is found in couplers, sealings, simulators, turbine components, scramjet combusting chamber, etc. Traditional machining process on these alloys with a good surface finish to a higher order of precision for attaining their outstanding characteristics make difficult, laborious, and expensive to apply. Advanced machining plays an important role in reckoning properties of the alloys, saving labor, production cost, quick and simplification of the process to be implemented.

One of the significant characteristics of alloys of low thermal conductivity materials is undergoing Strain hardening in Nickel and Titanium-based alloys, Super and shape memory alloys, etc. as they are complicated to apply fixed machining processes like turning, drilling, boring, milling, etc., as well as causing excessive wear and sticking of chips on the tool. Various advanced machining processes like ECM (electro-chemical), EDM (electro-discharge), AJM (abrasive-jet), WEDM (wire-electro-discharge), laser, hybrid machining processes, etc. in which WEDM has proved most adaptable un-conventional machining procedures to hard metals and their alloys in any proportions forming different alloys discharging is affected by breakdown voltage as the wire (made of Cu, brass, Mo, Al, and Graphite) is bolstered through workpiece [2]. Graphite wire because of its high melting point temperature Material Removal rate (MRR) is higher compared to Cu wire, which increases hardness due to Titanium carbide developed on the surface. In contrast, the Aluminium wire provides a good surface finish. As WEDM develops high temperature procedure produces reformed and subdued surfaces affected by heating introduce residual tensile stresses, causing rupture [3, 4]. The surfaces produced with short and long pulses of discharge current had shown the same surface roughness even with the constant pulse energy. Still, the distribution of surface finish found different [5, 6]. Response features (MRR and SR) on input factors of shape memory alloy (Ti50Ni42.4Cu7.6) were investigated.

A combination of low values of maximum-current (C) and instant Pulse-on-duration (P) become more helpful for maximizing MRR than to minimize SR with a large amount of Pulse on duration is needed. The effect of WEDM factors during machining the Ti50Ni49Co1 surface of SMA developing poor surface quality at a higher value of P and rich surface finish at high speed. Response surface methodology (RSM) for modeling and optimizing WEDM factors of Nickel-based superalloy using the desirability approach has been carried out [7]. On Nimonic-80A, optimization of MRR and wear a fraction of wire using Taguchi with performed experiments of the WEDM process [8]. RSM optimization of the outputs of SR and measurement variation of the WEDM process used in pure titanium performed [9, 10].

The fuzzy controller, along with its magnificent economic algorithm for handling the intricacies in solving regular manufacturing optimization challenges, was suggested [11, 12]. But surveys of the sources show no systematic studies of the input factors affecting the surface finish and MRR through the WEDM process applied on Nitinol (Nickel-Titanium) alloy. Consequently, this study emphases evaluating the effect of input factors, namely P, Q, C, and V, on Nitinol alloy machining characteristics (MRR and SR). So, in current research, the plan of the experiment was prepared with CCD standards to elucidate the combined impact of factors on response features of Nitinol alloy consuming electrode wire made of "molybdenum." Hence, important regression models were generated for investigating the influence of P, Q, C, and V on responses utilizing RSM involved higher degree models. Optimization essentially looks for the probable superior set of factors either for maximizing/ minimizing the responses [13]. Various ways of optimizing the input factors of other processes and WEDM have been employed in the earlier work for single/multiple responses, namely, Taguchi design, RSM, Grey relation approach. Such techniques can suitably handle the single optimization response but not for multi-factor multi objectives as their results contradict in concluding [14]. In 1995, Kennedy and Eberhart offered PSO technique as a tool for transforming evolutionary procedure to the optimization of the performance characteristics very first time [15]. The PSO algorithm used for solving reliable non-linear updating problems after recognizing the actions of the ecological swarm bird returning to settle back, which detected in several categories of aerial organisms [16]. PSO generates top score measures within a short estimation time, as well as a

steady combination of factors [17]. Since the capability of the PSO system for executing the top score of the process, many engineers/researchers realize it as a fruitful decision over many issues, especially while managing multiple-goal updating matters [18].

Advanced and evolving procedures attaining success in solving multi-dimensional objectives with several confined targets and one of them is the PSO approach (stochastic optimization) which make use of a population of random solutions to search the optimum one from the various generations developed by initial community similar to management of a bird flock. It falls in the category of evolution algorithms like a statistical search mechanism. Additionally, the PSO is extending to deal with multi-objective optimization (MOO) problems, and PSO procedures are easy to implement due to their simple mathematical and logical operators, which make itself computationally less complicated [19]. Swarm information is considered as a genetic, and artificial intelligence depends on the joint performance in regionalized self-prepared structures.

Excellent surface finish and the high metal removable rate of Nitinol alloy is a stimulating topic in the field of production. The study available on this WEDM machining method is limited. In this scenario, the prevailing study is on investigating the impact of factors on machining characteristics (SR and MRR). Furthermore, multi-output/ objective PSO involving genetic algorithm with multi outputs along with Pareto font is applied to acquire the top-scored optimum set of factors for maximizing and minimizing the MRR and SR, respectively. Presently no research work about the application of PSO for multi objectives of the WEDM method of Nitinol alloy. Using a set of strategic trials, the fitness function to optimize responses were changed in the mathematical model form and using ANOVA, the importance of it in the way of the RSM model is examined. The optimum setting of WEDM process factors was achieved by employing a multi-output genetic algorithm based PSO, and PSO performances of Pareto front solutions were compared and validated.

Materials And Methods

Workpieces made of commercially available material Nitinol alloy (Nickel-Titanium alloy) were prepared for machining using WEDM. The development of numerical models is very critical in the production process to develop parts in a short time at the lowest machining cost. The realistic model using RSM can develop a compromising relationship of input factors and responses [11]. In RSM, the noticeable interaction between input factors and output is expressed as follows.

$$Z = h\ (a1; a2; a3 \ldots\ldots\ldots\ldots\ldots\ldots\ an) + error \quad (1)$$

Where Z, the output characteristic to be optimized and h, the objective function consists of both dependent and independent factors a1, a2, a3 . . . . . an, along with fixing errors. The optimization of WEDM factors involved in the machining of an Aluminium alloy 5754 produced by friction-stir-welding using the Taguchi design method, for experimentation planning in an orthogonal array format to take all various possible combinations of factors and their levels . To improve the quality and accuracy of the WEDM process, Taguchi parametric design and RSM were employed. In this attempt, face-centered composite design (CCD) was used to develop mathematical models for the MRR and SR and to study parameters influence on accuracy. RSM seems to be a suitable method to analyze and optimize the input factors. This method increases not only efficiency but also product authority [8, 9, 20]. The process factors influencing significantly on the MRR and SR responses are Pulse-on-duration, P, Pulse-off-duration, Q, maximum-Current, C, and Voltage, V. Table 1 details the chosen process factors at the various range.

Table 1.

The mathematical model using RSM will be used to develop the fitness function required for the PSO technique. In PSO, Multi-object optimization, along with a genetic algorithm, will be performed by MATLAB optimization toolbox using Pareto front solver.

Experimental Details

All trials on Nitinol parts using CNC Wire cut EDM were carried out, having a 0.2 mm diameter wire made of molybdenum (Mo) as electrode material. Mo wire has various advantages like high molten temperature as well as ultimate strength while producing complex shapes parts of aerospace and missile. Care must be taken about the wire diameter and the deionized water's pressure to use it as a dielectric liquid, keeping at around 2.6 kg/cm2, which should not vary. The trials were collected targeting CCD full fraction for all factor combinations occurring at higher (3) and lower (1), i.e., two levels and multi-responses (MRR and SR) of the WEDM process were tabulated in Table 2.

$$\mathrm{MRR\ (mm3/\ min)} = \frac{Volume\ (length*width*depth\ of\ cut)of\ material\ removed\ (mm3)}{\mathrm{Machining\ time\ (min)}} \quad (1)$$

Where the Measurement of Surface roughness is done by employing the surface roughness tester (Taylor Hobson profilometer) conducting at three different portions of the surface, and the average value of it presented in micrometers.

Table 2.

Multi-Objective Optimization (MOO) using PSO

Every particle in the group having a velocity vj(f) with that it can flee into the illustration area and can be characterized by a velocity vj(f) and position xj(f) vector. Their elements are well-expressed by the various input factors in the optimizing process. Modifications of the particle location are done by employing its preceding position data and its present velocity. Thus

$$vj(f+1) = j(f) + c1rand1\ (Pbestj - xj(f)) + c2rand2\ (Gbestj - xj(f)) \quad (2)$$

$$xj(f+1) = j(f) + vj(f+1) \quad (3)$$

Where vj(f) and xj(f) are the velocities and current position at iteration f; Pbestj and Gbestj are the personal and the global best position of particle j respectively; rand, w, c1, and c2 are the random number (from 0 to 1), the weighting function, the cognition, and social learning rate respectively.

The random numbers produce velocities updated in PSO are statistical may instigate an uncontrollable rise in velocity as well as the uncertainty of the search algorithm. This is prevented using the Pareto front algorithm along with a genetic algorithm by carrying out multi-objective PSO.

Multi-objective states yield an optimum set of solutions for input factors in the place of a single solution. They often include disagreeing responses such that one objective gets improved by causing a decline in solution. Two universal methods to MOO either by combining each objective function into a solo compound function or change entirely, leaving one response to the constraint group. The key gain of such a “weighted-sum” method is allowing an open application as well as numerically effective. The second universal method is to establish a complete Pareto front-optimum solutions group or an illustrative subgroup. The solution that can improve any response by deteriorating individual or more responses is known as nondominated (ND) solutions. The purpose of executing a MOO is to obtain a set of ND solutions, stabilizing the transaction among disagreeing responses called a Pareto set. The proposed work involves maximizing MRR along with minimizing SR.

Results And Discussion

Influence of Input factors on Responses MRR and SR

Experimental results obtained based on CCD were investigated to find the influence of various input factors on the responses (MRR and SR) using ANOVA at 0.05 level significant. ANOVA for MRR and SR (refer to Table 3 and 4) with the small value of probability indicates a larger value of correlation coefficient. According to the RSM investigation, the quadratic model used is statistically significant for both MRR and SR. The “coefficient of determination” R2 attaining 1 indicates the output characteristics fitting the real data, and this even helps in checking predicted and adjacent R2 (i.e., Pred-R2 and Adj-R2) reached unity. Above 90% for R2 as well as Adj-R2 of both machining characteristics (MRR and SR) shows that the mathematical model developed by regression has a good relationship between process factors and output results. The inputs like P, square terms - CXC, and interaction terms-PxC, are found to be most significant. V, Q, and C are found to an insignificant process parameter for MRR. Similarly, the ANOVA table for SR shows that C, P, and Q, and square term-CxC are essential to process parameters. V is found to be insignificant input factors for SR.

Table 3.

Table 4.

Figure 1.

Pareto charts also indicate most significant and significant factors at individual, square and interaction levels of factors as shown in Figure 1 (a) for MRR and (b) for SR.

Figure 2.

Figure 2 shows the 3D surface plot of output MRR varying to the level of input factors, and each Figure 2a to 2f shows the role of interaction of A, B, C, and D on MRR. The MRR decreases more with increased C and less with Pulse on time. That means an increase in C (from 2 to 4A) may severely decrease the MRR without even increasing the Pulse on time as it encourages swift melting along with alloy vaporization. But

the mid-side value of C might improve MRR up to A=37.5 µs and remains same up to 45 µs and then MRR increase further irrespective of A and C change after 45 µs because high value of C directs a large amount of energy hooked on the targeted area to remove the higher amount of metal along with impulsive forces in the dielectric fluid for taking away molten metal of targeted area. The MRR also gets increased due to change of shape as well as the size of surface pits, pores, etc., with an increase in C., whereas factors B and D have a counter effect on MRR, i.e., they contribute to MRR value only if A and C are also changing. The interactions of the input factors on SR are depicted in Figures 3 (a) to (f). At a low value of C, SR reduces with increasing A because of low impulsive forces retaining longer time. But at higher C, SR increases along with the A because high impulsive forces along with sparks and maintaining a more extended time would damage the surface, and hence SR increases. The pits, pores increase due to the high rate of erosion of an alloy. It is also noticed that low thermal conductivity and melting point gives a higher SR . The decisive empirical formed equations of machining characteristics (MRR and SR) are characterized in Eq. (4) and (5).

$$MRR = 6.30 - 0.0971\,P + 0.426\,Q - 1.923\,C - 0.033\,V + 0.000144\,P2 - 0.01338\,Q2 + 0.4116\,C2 + 0.00067\,V2 + 0.000548\,P*Q + 0.01060\,P*C + 0.000523\,P*V - 0.0390\,Q*C - 0.00094\,Q*V - 0.01224\,C*V \quad (4)$$

$$SR = 2.58 + 0.0067\,P + 0.0283\,Q + 1.195\,C - 0.1198\,V - 0.000240\,P2 - 0.00189\,Q2 - 0.1595\,C2 + 0.00122\,V2 - 0.000377\,P*Q + 0.002193\,P*C + 0.000023\,P*V + 0.00271\,Q*C + 0.000136\,Q*D + 0.00146\,C*V \quad (5)$$

Multi response optimization using RSM

To increase the WEDM performance, optimum factors set have to be selected by considering the responses such as high MRR and low SR, which are very difficult to get for achieving high-quality surface. For this, composite desirability (cd) approach is a most suitable technique for optimizing input factors to satisfy the conditions of responses by using a response function which determines the scale-free value (di) of the responses called desirability (lies between 0 to 1) expresses the zero and absolute issues for the responses which are at outer allowable margins. Whereas cd is the weighted statistical average of the distinct desirability of responses.

Figure 3.

The optimum factors with the greatest desirability will be chosen for the mathematical models of MRR and SR by combining the objectives to satisfy the combined goals of all the responses. The optimality solution evaluates higher MRR and Lower SR and their corresponding predicted optimum input factors values presented in Table 6. The desirability need not always be equal to one, but its value discloses the proximity of the margins set pertaining to the real optimum values. An optimal set of factors using Minitab 19 software was evaluated and presented in Table 5. Once the optimum values are achieved, it becomes necessary to validate to check the confirmation with experiments at these optimal values. Table 6 gives % error for confirming with experimentation results of WEDM and found very small, which is acceptable by the researchers.

Table 5.

Table 6.

Figure 4.

The desirability gradient and line graph of the WEDM process (refer Figure 4) shows the di value obtained for each response generated between low and high values. If the targeted responses di value is closer to 1 show having good desirability, then the desirability is good. The global desirability D = 0.8748 shows closeness of responses to the target set.

Results of MOOPSO

The PSO technique was applied, keeping in mind that both should not be minimized as when SR reduces by minimizing the objective function, the MRR also gets reduced. But we need the maximization of MRR while minimizing the SR. To avoid conflict between objectives of MRR and SR and to achieve higher MRR and lower, the optimum set of input factors are to be located. Thus, the objective function of MRR is altered into minimization form in the following way as below:

Function 1= Minimize (1/MRR);

Function 2 = Minimize (SR).

To achieve MO optimization as per specific goal, a PSO toolbox of MATLAB program was employed to execute the source code of the anticipated algorithm. Distribution of Pareto front containing 100 optimum sets of factors satisfying the condition of both functions. Figure 5 showing the Pareto front distribution of top scored ND solutions out of the 100-optimum set of populations while performing optimizations of two functions. The best solution depends on product requirements or upon the choice of engineer for a specifically designed process. MOOPSO forecasted the finest results within levels of factors. Top scored solutions come from 100 top global solutions, but only the finest 25 solutions are provided in Table 6. After both analysis and comparing with empirical outputs of MRR using Pareto front, the maximum value of 3.5420068 mm3/min is found at pulse-on-duration of 25.1118229 µs, pulse-off-duration of 12.3503394 µs, C of 2.009124 amp and V of 45.120498 volts, with corresponding to experiment no. 27 in Table 2 where the maximum MRR = 3.5663.23mm3/min at pulse-on-duration =25 µs, Q = 14 µs, C = 14 amp, and V = 50 volts. The MRR of the Pareto front optimal solution exhibits their values are slightly lesser than the experiment results. Furthermore, the 3-D MRR output plot (referring Figure 5) reveals that the MRR decreasing as the Pulse on time and C increases. The proper combination of input factor levels may yield a higher value of MRR. It is also found that minimum MRR of 2.508 mm3/min (refer Table 2) in experiments having s.no. 11 at pulse-on-duration =35 µs , Q =14 µs, C =3amp, and V =45volts. while Pareto front provided the minimum value of MRR of 2.66760113mm3/min at pulse-on-duration = 49.83780 µs , Q = 13.8012141 µs, C = 2.00763 amp, and V =45.50042649.614 Volts. A comparison of the minimum MRR provides the Pareto front result is 0.13 mm3/min higher experimental one, which is highly acceptable, and this difference is because of the factor level changes.

Similarly, Pareto front results revealed the minimum SR of 1.4855502 µm at P = 4549.83780 µs, Q = 13.801214 µs, C = 2.00763 amp, and V = 45.500426 volts and experiment output no. 5 (refer Table 2), the minimum SR of 1.501µm at P = 50 µs, Q = 14 µs, C = 2 amp, and V = 50 volts is slightly lower than the Pareto front analysis. Furthermore, the 3D response plots of SR (Fig. 6) show that the SR decreases with the increasing values of P, V and C. Therefore, by proper levels of input, factors yield the minimum SR, which is need of an hour. Further, experimental output no. 9, the maximum SR of 2.615 µm at P = 25 µs, Q = 8 µs, C = 4 amp, and V = 40volts. While Corresponding results of Pareto front seen with the maximum SR of 1.7886815 µm at P = 25.1118229 µs, Q = 12.3503394 µs, C = 2.009124amp, and V = 45.1204989 volts. Comparing the maximum SR of experimental is 0.4 µm higher than Pareto optimal results (refer Table 7). This may be because of factors level differences between these two methods. The five most excellent pareto front results keeping minimum SR and maximum MRR are presented in the Table 8.

Table 7.

Table 8.

Figure 5.

Conclusions

The particle swarm optimization (PSO) and RSM techniques based on CCD experimental plan were employed for multi-response optimization of input factors of the WEDM method of Nitinol alloy has been studied in this research. Using a composite desirability approach, optimization carried out yielding empirical model for evaluating the role of input factors on multi responses (MRR and SR). The inferences were made on the results of different methods for maximizing MRR and Minimizing SR are as follow:

- Experimental values presented P and C are highly contributing factors to machining responses during maximization of MRR/ minimization of SR such that minimum level of P and C discharge quick energy (electrical type) for alloy melting and vaporization. This yields maximum MRR and minimum SR as impulsive forces developed would be of lower intensity.
- Composite desirability approach for optimizing the multi-responses yield the optimal combination for setting the level of factors for high MRR and Low SR very low percentage of error but acceptable are as follows: P = 25 µs, Q = 13.39 µs, C = 2.0 amp, and V = 48.59 volts.
- The Pareto front solution from MRPSO also shown the response MRR increase and SR decrease with decreasing P and C rather than Q and V.
- The MRPSO provided a vast combination of input factors in comparison to experimentation for allowing us to select very appropriate levels of factors to maximize MRR along with minimum SR for improving process efficiency.
- The proper combinations of both high and low levels P, Q, C, and V are more suitable for maximum and minimum of MRR, and SR has been presented using MOOPSO.
- The MRPSO presented a set of optimal solutions using the Pareto optimal front to enable the designers to have the set optimal solutions for selecting the optimal values of factors suitable for their product requirement.

Declarations

Availability of data and materials

The supporting data used and/or analyzed during the current study are available from the corresponding author on reasonable request.

Acknowledgements

Not applicable.

Funding

No Fund is available for this work.

Author information

Affiliations

Department of Mechanical Engineering, College of Engineering and Islamic Architecture, Umm Al-Qura University, Makkah city, Kingdom of Saudi Arabia.

Author's contribution

The authors participated in the conceptualization of the research. Mohammed Yunus and Mohammad S. Alsoufi prepared the data for experimentation and analysis. The authors participated in the analysis and interpretation of the data. Mohammed Yunus drafted the manuscript and figures are sketched by Mohammad S. Alsoufi. The authors revised the manuscript for intellectual content and approved the final manuscript.

Corresponding author

Corresponding to Mohammed Yunus and email: myhasan@uqu.edu.sa

Ethics declarations

Competing interests

The authors declare that they have no competing interests.

Table: Nomenclature

References

1. Srinivasan AV, McFarland DM (2002) Smart Structures: Analysis and Design. Meas Sci Technol 13(9):1502–1503
2. Lin HC, Lin KM, Cheng IS (2001) The electro-discharge machining characteristics of TiNi shape memory alloys. Journal of Materials Science 36(2):399–404
3. Abu Zeid OA (1997) On the effect of electrodischarge machining parameters on the fatigue life of AISI D6 tool steel. J Mater Process Technol 68(1):27–32
4. Merdan MAER, Arnell RD (1991) The Surface Integrity of a Die Steel after Electrodischarge Machining: 2 Residual Stress Distribution. Surf Eng 7(2):154–158
5. Chen SL et al (2008) Electrical discharge machining of a NiAlFe ternary shape memory alloy. J Alloy Compd 464(1):446–451
6. Liao YS, Yu YP (2004) Study of specific discharge energy in WEDM and its application. Int J Mach Tools Manuf 44(12):1373–1380
7. V C (2016) Response surface Methodology and Desirability Approach to Optimize EDM Parameters. International Journal of Hybrid Information Technology 9(4):393–406

8. Goswami A, Kumar J (2014) Investigation of surface integrity, material removal rate and wire wear ratio for WEDM of Nimonic 80A alloy using GRA and Taguchi method. Engineering Science Technology an International Journal 17(4):173–184
9. Kumar A, Kumar V, Kumar J (2013) Multi-response optimization of process parameters based on response surface methodology for pure titanium using WEDM process. The International Journal of Advanced Manufacturing Technology 68(9):2645–2668
10. Berkani S et al (2015) Modeling and optimization of tool wear and surface roughness in turning of austenitic stainless steel using response surface methodology. Materials Science Engineering 9(1):63–74
11. Khaled AA, Hosseini S (2015) Fuzzy adaptive imperialist competitive algorithm for global optimization. Neural Comput Appl 26(4):813–825
12. Garg MP, Kumar A, Sahu CK (2017) Mathematical modeling and analysis of WEDM machining parameters of nickel-based super alloy using response surface methodology. Sadhana 42(6):981–1005
13. Chenthil Jegan TM, Ravindran D (2017) Electrochemical machining process parameter optimization using particle swarm optimization. Comput Intell 33(4):1019–1037
14. Chakala N, Chandrabose PS, Rao CSP, Optimisation of WEDM parameters on Nitinol alloy using RSM and desirability approach. Australian Journal of Mechanical Engineering, 2019: p. 1–13
15. Kennedy J, Eberhart R. Particle swarm optimization. in Proceedings of ICNN'95 - International Conference on Neural Networks. 1995
16. Kalayci CB, Gupta SM (2013) A particle swarm optimization algorithm with neighborhood-based mutation for sequence-dependent disassembly line balancing problem. The International Journal of Advanced Manufacturing Technology 69(1):197–209
17. Jia Q, Seo Y (2013) An improved particle swarm optimization for the resource-constrained project scheduling problem. The International Journal of Advanced Manufacturing Technology 67(9):2627–2638
18. Yildiz AR, Solanki KN (2012) Multi-objective optimization of vehicle crashworthiness using a new particle swarm based approach. The International Journal of Advanced Manufacturing Technology 59(1):367–376
19. Prakash C et al, Multi-objective Optimization of MWCNT Mixed Electric Discharge Machining of Al–30SiCp MMC Using Particle Swarm Optimization, in Futuristic Composites: Behavior, Characterization, and Manufacturing, S.S. Sidhu, et al., Editors. 2018, Springer Singapore: Singapore. p. 145–164
20. Bhushan RK (2013) Optimization of cutting parameters for minimizing power consumption and maximizing tool life during machining of Al alloy SiC particle composites. J Clean Prod 39:242–254

Tables

Table 1. Process input factors and their levels

	Coded		Levels		
S. No.	Factor	Parameters	1	2	3
1	P	Pulse-on-duration µs	25	35	50
2	Q	Pulse-off-duration µs	8	11	14
3	C	Maximum-Current Amp.	2	3	4
4	V	Voltage Volts	40	45	50

Table 2. Experimental orthogonal array design and corresponding results

P	Q	C	V	Material Removal Rate (mm^3/min)	Surface Roughness (µm)
3	3	3	3	2.6296	2.394
3	3	3	1	2.65335	2.413
3	3	1	1	2.51275	1.52
3	1	1	3	3.3649	1.8145
3	3	1	3	2.73695	1.501
2	2	2	3	2.70275	2.28
2	2	2	2	2.7113	2.318
1	3	3	1	3.06945	2.584
1	1	3	1	3.4523	2.6125
3	2	2	2	2.64575	2.1185
2	3	2	2	2.508	2.204
2	1	2	2	2.62295	2.299
2	2	2	2	2.5916	2.318
1	2	2	2	2.8291	2.3275
2	2	2	2	2.7797	2.413
3	1	3	1	2.8196	2.508
2	2	2	2	2.78065	2.337
2	2	3	2	3.0761	2.546
1	1	3	3	3.1996	2.5935
1	1	1	1	3.25375	1.881
2	2	2	2	2.73125	2.318
2	2	2	2	2.6182	2.3275
2	2	1	2	3.11885	1.672
3	1	1	3	2.47665	1.596
2	2	2	1	2.70275	2.318
1	3	3	1	3.4694	1.786
1	3	3	3	3.5663	1.7575
3	1	3	1	2.40255	1.653
3	1	3	3	2.8196	2.489
1	3	3	3	2.8633	2.5745

Table 3. ANOVA table for MRR

Basis	Degree of Freedom	Adj-Sum of Squares	Adj- Mean Squares	*F*-value	*P*-value	
Model	14	2.72112	0.19437	12.57	0.000	
Linear	4	1.53423	0.38356	24.81	0.000	
P	1	1.52466	1.52466	98.63	0.000	Significant
Q	1	0.00820	0.00820	0.53	0.478	
C	1	0.02251	0.02251	1.46	0.246	
V	1	0.00004	0.00004	0.00	0.960	
Square	4	0.91195	0.22799	14.75	0.000	
P^2	1	0.00132	0.00132	0.09	0.774	
Q^2	1	0.03858	0.03858	2.50	0.135	
C^2	1	0.45050	0.45050	29.14	0.000	Significant
V^2	1	0.00075	0.00075	0.05	0.828	
Two-Way Interaction	6	0.55061	0.09177	5.94	0.002	
P x Q	1	0.00615	0.00615	0.40	0.538	
P x C	1	0.24869	0.24869	16.09	0.001	Significant
P x V	1	0.01557	0.01557	1.01	0.332	
Q x C	1	0.21787	0.21787	14.09	0.002	
Q x V	1	0.00302	0.00302	0.20	0.665	
C x V	1	0.05957	0.05957	3.85	0.068	
Error	15	0.23187	0.01546			
Lack of Fitness	10	0.19949	0.01995	3.08	0.113	
Fundamental Error	5	0.03238	0.00648			
Total	29	2.95299				

Model Summary of MRR

S	R-squared	R-squared (adjusted)	R-squared (predicted)
0.104330	92.15%	90.82%	84.38%

Table 4. Analysis of variance table for SR

Basis	Degree of Freedom	Adj-Sum of Squares	Adj-Mean Squares	F-value	P-value	
Model	14	3.64511	0.26037	149.83	0.000	
Linear	4	3.32368	0.83092	478.17	0.000	
P	1	0.15273	0.15273	87.89	0.000	Significant
Q	1	0.02758	0.02758	15.87	0.001	
C	1	2.98655	2.98655	1718.68	0.000	Significant
V	1	0.00457	0.00457	2.63	0.126	
Square	4	0.21599	0.05400	31.07	0.000	
P^2	1	0.00365	0.00365	2.10	0.168	
Q^2	1	0.00077	0.00077	0.44	0.516	
C^2	1	0.06765	0.06765	38.93	0.000	Significant
V^2	1	0.00248	0.00248	1.42	0.251	
Two-Way Interaction	6	0.01580	0.00263	1.52	0.239	
P x Q	1	0.00290	0.00290	1.67	0.216	
P x C	1	0.01064	0.01064	6.12	0.026	
P x D	1	0.00003	0.00003	0.02	0.899	
Q x C	1	0.00105	0.00105	0.60	0.449	
Q x V	1	0.00006	0.00006	0.04	0.851	
C x V	1	0.00085	0.00085	0.49	0.495	
Error	15	0.02607	0.00174			
Lack of Fitness	10	0.01913	0.00191	1.38	0.380	
Fundamental Error	5	0.00693	0.00139			
Total	29	3.67118				

Model Summary of MRR

S	R-squared	R-squared (adjusted)	R-squared (predicted)
0.0416857	99.29%	98.63%	98.19%

Table 5. Optimum values of Nitinol alloy

Factors	A	B	C	D
Levels	25	13.3861	2	48.5859

Table 6. Predicted and observed values of Nitinol alloy

				Predicted		
Response		Observed	SE Fit	95% CI	95% PI	Error (%)
SR	Minimize	1.7618	0.0331	(1.6912, 1.8324)	(1.6484, 1.8753)	1.5
MRR	Maximize	3.5662	0.0988	(3.3556, 3.7767)	(3.2277, 3.9046)	2.5

Table 7. Few Pareto front solutions of MRPSO

		BE	C	D	SR	MRR
1	25.1118229	12.3503394	2.009124	45.120498	1.7886815	3.5420068
2	26.3527045	13.5577625	2.005825	45.559656	1.7556562	3.46765
3	40.5901393	13.556345	2.005689	45.5593612	1.6270165	2.970345
4	44.2577660	13.623444	2.004210	45.6723322	1.5748247	2.85222
5	41.372580	13.632751	2.005639	45.504659	1.615188	2.94130952
6	25.139723	13.565896	2.007550	45.6149662	1.762997	3.5107027
7	29.943054	13.552877	2.000158	45.716168	1.727940	3.3438364
8	30.842303	13.568946	2.005914	45.455762	1.725763	3.3032148
9	47.516891	13.632021	2.007591	45.6219439	1.52834	2.74627547
10	39.339483	13.582901	2.007125	45.2547781	1.643595	3.0060108
11	28.36971	13.632919	2.00671	45.4713454	1.7426199	3.3889483
12	27.66276	13.560233	2.007347	45.6554528	1.748633	3.4182121
13	43.27807	12.983334	2.000026	45.2635824	1.6037521	2.8990178
14	49.83780	13.8012141	2.00763	45.500426	1.4855502	2.66760113
15	38.35412	13.464438	2.00110	45.554622	1.6526097	3.052191
16	35.93012	13.634225	2.00632	45.626082	1.67812964	3.12372824
17	38.680602	13.589088	2.00633	45.554353	1.64955087	3.03180880
18	47.918069	13.722225	2.007098	45.327659	1.51976365	2.72664270
19	45.3503468	13.475613	2.004385	45.4988402	1.56379364	2.81986745
20	46.4554287	13.740341	2.004998	45.460131	1.540144	2.7750993
21	32.6452667	13.6179144	2.007574	45.508611	1.710838	3.2359589
22	25.1265469	12.7423078	2.008351	45.2686245	1.780761	-3.5363104
23	26.8341290	13.5680084	2.005942	45.573252	1.752719	-3.4493672
23	48.2690753	13.7415251	2.007302	45.344606	1.513625	2.71524689
25	37.0194402	13.6473782	2.007617	45.4665371	1.6678021	3.08331782
26	37.2760105	13.5648563	2.006178	45.668391	1.6654667	3.08127597

Table 8. Best five optimum solutions of MRPSO after confirmation test

Run order	A	B	C	D	SR	MRR
1	25.1118229	12.3503394	2.009124	45.120498	1.7886815	3.5420068
7	29.943054	13.552877	2.000158	45.716168	1.727940	3.3438364
9	47.516891	13.632021	2.007591	45.621944	1.52834	2.7462755
10	39.339483	13.582901	2.007125	45.254778	1.643595	3.0060108
14	49.83780	13.8012141	2.00763	45.500426	1.4855502	2.66760113

Table Nomenclature

P	Pulse-on-duration
Q	Pulse-off-duration
C	Maximum-current
V	Voltage
MRPSO	Multi-Response Particle Swarm Optimization
SR	Surface roughness
WEDM	Wire electro discharge machining
ANOVA	Analysis of variance
ECM	Electro- Chemical Machining
EDM	Electro Discharge Machining
AJM	Abrasive Jet Machine
RSM	Response surface methodology
Al	Aluminium
SMA	Shape Memory Alloy

Figures

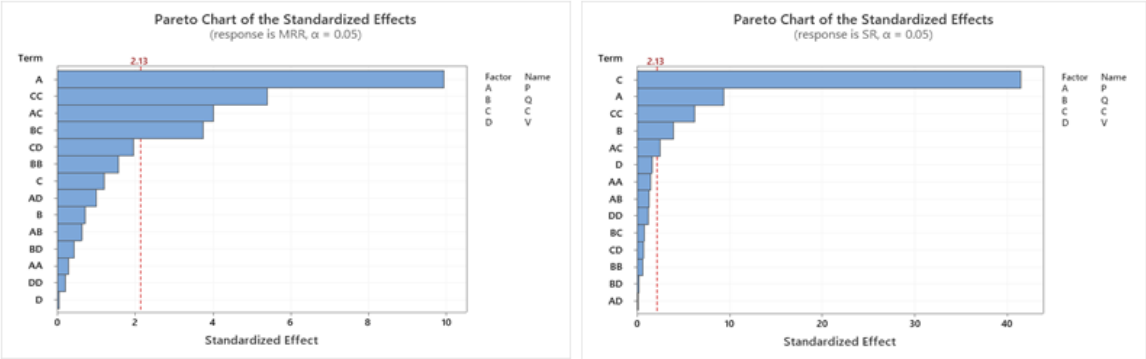

Figure 1

Pareto charts for input factors on response (a) MRR (b) SR

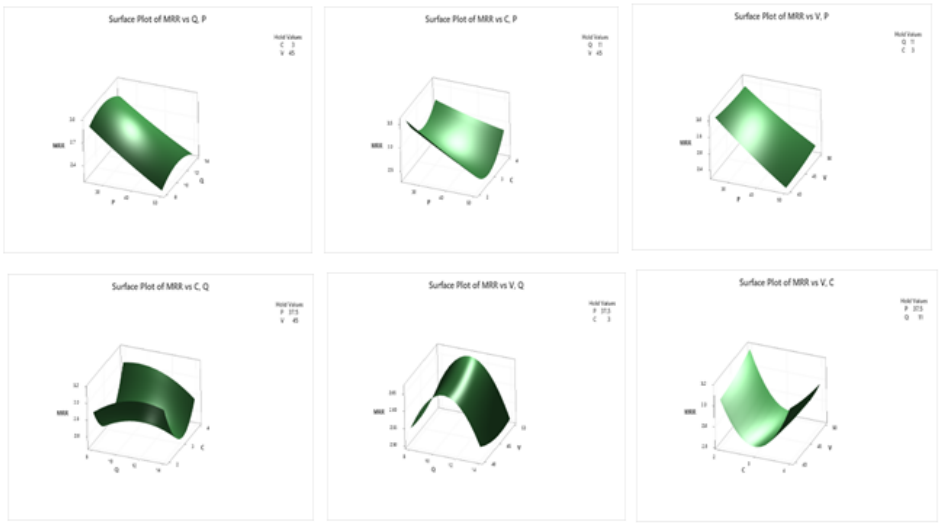

Figure 2

3D Response plot of MRR vs (a) Q & P (b) C &P (c) V &P (d) C & Q (e) V & Q (f) V &C

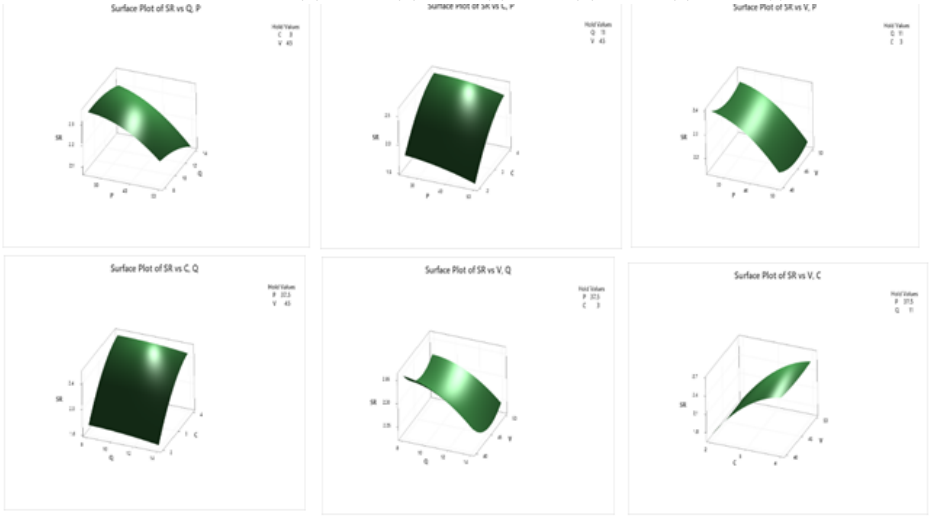

Figure 3

3D Response plot of response SR vs (a) Q & P (b) C &P (c) V &P (d) C & Q (e) V & Q (f) V &C

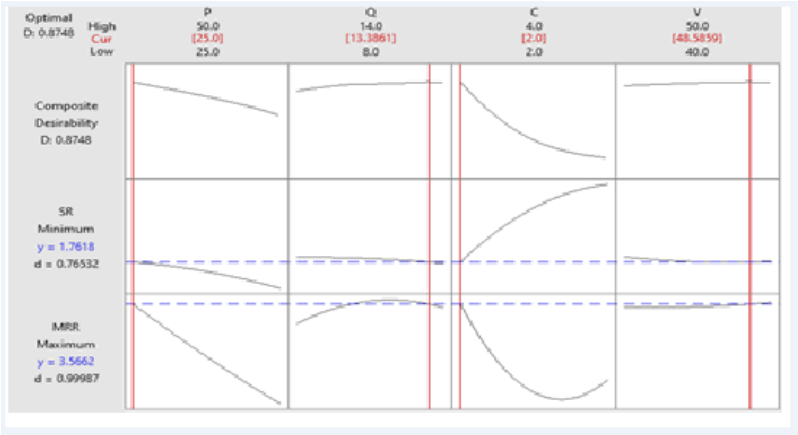

Figure 4

Desirability and optimal for input and responses

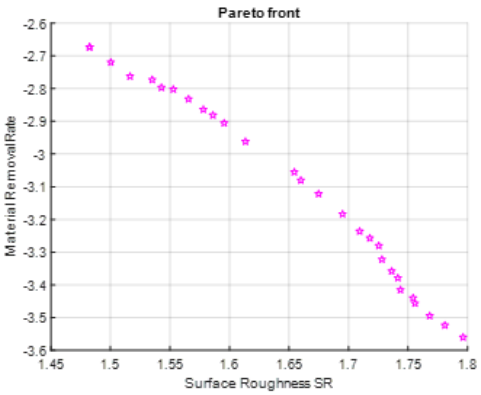

Figure 5

Pareto optimal front diagram of two responses using MRPSO